Hindawi
Scientific Programming
Volume 2022, Article ID 2449504, 10 pages
https://doi.org/10.1155/2022/2449504

Research Article

Optimization Method of High-Precision Control Device for Photoelectric Detection of Unmanned Aerial Vehicle Based on POS Data

Xuebin Liu,[1,2] Hanshan Li ,[3] and Suiming Yang[4]

[1]*School of Mechatronic Engineering, Xi'an Technological University, Xi'an 710021, Shaanxi, China*
[2]*Department of Economic Management, Tianfu Information Vocational College, Meishan 620564, Sichuan, China*
[3]*School of Electronic and Information Engineering, Xi'an Technological University, Xi'an 710021, Shaanxi, China*
[4]*Traffic Engineering College, Xi'an Traffic Engineering Institute, Xi'an 710000, Shaanxi, China*

Correspondence should be addressed to Hanshan Li; 1764100164@e.gzhu.edu.cn

Received 22 July 2022; Revised 27 August 2022; Accepted 9 September 2022; Published 25 September 2022

Academic Editor: Juan Vicente Capella Hernandez

With the rapid development of modern technology, due to the light-weight, small size, and good concealment, unmanned aerial vehicle (UAV) has received much attention from the society and has been vigorously promoted. Photoelectric tracking detection system is an important means in the field of modern detection. The combination of a UAV and photoelectric detection system can effectively play an important role in reconnaissance and exploration, target positioning, communication, and navigation. At present, the relevant personnel have higher and higher requirements for the accuracy of the photoelectric detection function of UAV, and the original POS data relied on by the existing photoelectric detection devices of UAV has systematic errors, which leads to the low accuracy of photoelectric detection control. Therefore, in order to achieve the purpose of improving the high-precision control of the photoelectric detection device of UAV, this paper designed an optimization method for the high-precision control device of photoelectric detection of UAV based on POS data. Firstly, the improved PID control algorithm is applied to the optimization of the UAV control device, and secondly the error correction model is established by analyzing the error source, and the original POS data is corrected by the model. This paper used the designed high-precision control device optimization algorithm and the traditional algorithm to compare the stability control experiments of the UAV platform, respectively. The experimental results showed that the application of the improved UAV photoelectric detection control device optimization method could effectively improve the control device optimization accuracy of UAV photoelectric detection by 8.23%, which was conducive to the efficient implementation of the project.

1. Introduction

The rapid development of POS data systems and photoelectric detection provides new means for obtaining specific geographic information. Combining POS data-based UAVs with photoelectric detection can greatly reduce the difficulty of surveying a large number of surface control points. In addition, by using this method, three-dimensional spatial data can be acquired quickly and in real time. However, the current photoelectric detection work has put forward higher requirements for obtaining high-resolution three-dimensional spatial data in various regions. The current control device is not optimized enough to meet the demand. In this reality, POS data and drones are combined for photoelectric detection. The high-precision control device for photoelectric detection of drones based on POS data is optimized. This has positive practical significance for the development of the UAV photoelectric detection industry.

Now, there are some research studies on the photoelectric detection of UAVs by scholars: the research of He et al. proposed an analysis method to improve the photoelectric detection accuracy of UAVs. Firstly, the UAV assembly accuracy was comprehensively modeled and simulated using kinematic analysis of homogeneous coordinate transformation. Then, by

analyzing the manufacturing process, the shaft perpendicularity, runout, and assembly errors of the gyroscope were defined and modeled, which improved the photoelectric detection accuracy of the UAV [1]. By using drones, Escobar and Sandoval obtained 8,000 images with a spatial resolution of 1.40 cm on a 30-kilometer beach. These images were used to construct an orthomosaic to detect and analyze turtle shell bones using object-based images [2]; the goal of Ren and Jiang is to design a system for automatically distinguishing targets using drones. He proposed a method of regularizing two-dimensional complex numbers for Fourier transform to solve the problem of target discrimination [3]. Thomas et al. used a multispectral camera on a fixed-wing drone to acquire high-resolution images. Three spectral textures and four detection classifiers were used to identify objects. Finally, the detection accuracy reached 96% [4]. Damian et al. proposed an automatic identification method for UAVs which was used to detect the multispectral image data obtained by UAVs and analyzed the existing sun reflection problem [5]. Kerrache et al. proposed an intelligent malicious behavior detection scheme based on adaptive detection threshold technology. In addition to detecting malicious nodes, the solution also relied on UAVs' photoelectric detection to deal with various negative effects of the detection process [6]. Martinez and Barczyk applied cascade classifiers to the photoelectric detection of UAVs and developed a computer vision algorithm for detecting pedestrians in videos, which had excellent performance in various environments [7]. The abovementioned research study analyzed the related application and development of UAV photoelectric detection.

In addition, many scholars have conducted research on POS data. Li et al.'s research introduced the working principle and components of airborne POS. Some key technologies of airborne POS were summarized, which included error calibration and compensation, initial alignment, lever arm error modeling, time synchronization, and comprehensive estimation methods [8]. Niu et al. proposed a novel indoor pedestrian POS data solution that could provide continuous localization through the correction of control points to maintain its absolute high accuracy [9]. Ye et al. proposed a distributed positioning system based on POS data. Firstly, based on the multidimensional requirements of flexible deformation information, the layout scheme of POS data was designed. Then, the POS data was quadratically fitted to obtain continuous strain, deformation displacement, and angle. The final experimental results showed that the positioning accuracy of the distributed positioning system based on POS data has been significantly improved [10]. Jianli proposed a second-order adaptive dual-filter smoother for solving nonlinear problems in POS data systems, which could adaptively estimate noise covariance in real time. The vehicle experiment results showed that this method could improve the attitude accuracy of the distributed POS data system by 27.84% [11]. Gong and Chen proposed a Kalman filter for the accuracy and real-time performance of the data transmitted by the airborne distributed positioning system. The state variables of the transfer-aligned nonlinear mathematical model were divided into two groups. One group was linear variables independent of nonlinear variables, and the other group was composed of nonlinear variables and coupling of linear variables [12]. Zhu et al. proposed a new real-time gravity compensation method, which took the gravity disturbance as the error state of the POS Kalman filter. An accurate gravity disturbance model was established based on the time-varying Gauss–Markov model [13]. Takashima et al. studied the integration of POS data into an imperfect in-vehicle automation system to reduce the negative impact of human-robot collaboration perception [14]. Langbehn et al. studied imperceptible camera motion by synchronizing POS data with the human visual process, especially to achieve position and orientation redirection [15]. The abovementioned studies have carried out a certain degree of effective research on POS data.

In recent years, UAVs have developed rapidly with the advantages of low cost, strong survivability, and good maneuverability. The method of photoelectric detection work by unmanned aerial vehicles is gradually becoming popular. Therefore, this paper designed a high-precision control device optimization method for UAV photoelectric detection based on POS data, which was conducive to better development of UAV photoelectric detection work.

2. UAV Photoelectric Detection Optimization Method

2.1. UAV and Photoelectric Detection. As a new type of aircraft, UAV has developed rapidly in recent years, and its technology has become more and more mature [16]. Drones have the following notable advantages:

(1) Strong concealment: UAVs do not need pilots, so UAVs are small in size and light in weight, which is of great help to improve the concealment of UAV reconnaissance. The improvement of concealment helps to avoid interference from other sources in the process of performing photoelectric detection. Therefore, the security is greatly improved.

(2) Flexible mobility: the design structure of the UAV is relatively simple. After setting the automatic navigation, the flight is controlled by the computer and will not be affected by the weather at all. There is no need to consider the carrying capacity of the driver in the design; only the ultimate carrying capacity of the UAV material needs to be considered. In this way, the performance advantages of the UAV can be maximized and the maneuverability of the UAV application can be greatly improved. High maneuverability enables drones to perform difficult maneuvers in a variety of environments, which enables drones to explore places that humans cannot.

(3) Cost saving: UAV is small in size and consumes less raw material. Drones consume far less fuel and material than manned aircraft. The cost of drones is only a few percent of that of manned aircraft, and the training of operators is relatively simple, which saves a lot of money.

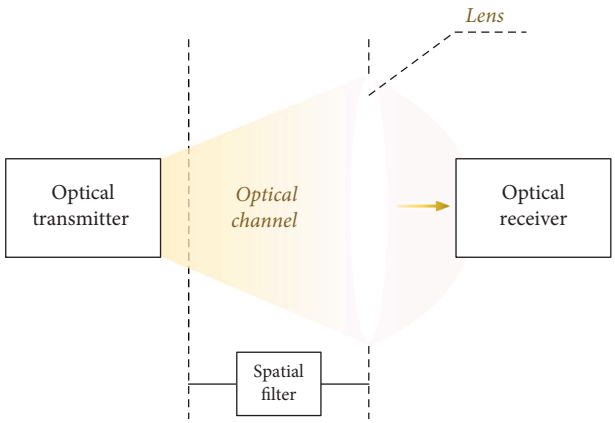

Figure 1: Photoelectric detection system.

In modern society, with the development of science and technology, photoelectric detection plays an increasingly important role [17]. From a professional point of view, photoelectric detection refers to the use of radar, computers, sonar, optical instruments, and other equipment to evaluate the location, properties, and types of targets [18]. The most important functional module in photoelectric detection is target recognition, and its basic principle is to analyze the echoes reflected by the target. Detected targets are identified based on phase, amplitude, polarization, spectrum, and so on [19]. In the military field, photoelectric detection technology can provide detailed battlefield conditions in the process of cooperative operations of various participating units on the battlefield. Photoelectric detection technology plays an important role in accurately estimating the war situation, formulating combat plans, and correctly commanding operations.

Compared with the electronic detection system, the carrier frequency element of the photoelectric detection system has been improved several times in the order of magnitude. Since the power of the carrier frequency can be superimposed and amplified, the number of carrier frequency components can reflect the performance of the photoelectric detection system to a certain extent. This change in carrier frequency has made a qualitative leap in the implementation of optoelectronic systems and has also undergone a qualitative change in function. The basic model of the photoelectric detection system is shown in Figure 1.

In the photodetection process, the reception of the optical signal is very important [20]. Generally speaking, when an optical signal emitted by an optical transmitter undergoes a series of transmissions, its amplitude will be affected and attenuated. In addition, the pulse waveform of the optical signal is also expanded. The function of the optical receiver is to detect the transmitted weak optical signal, and the received incident light field is amplified, shaped, and regenerated into the original transmission signal. Finally, the information from the optical carrier is recovered. The optical receiver generally consists of three parts: the light receiving front end, the photodetector, and the subsequent processing circuit. The light-receiving front end is composed of an optical receiving system composed of a lens and a light collecting part. The photodetector focuses the light received by the optical receiving system on the photosensitive surface of the photodetector and converts the optical signal into an electrical signal. The subsequent processing circuit amplifies, filters, and processes the electrical signal converted by the photodetector and recovers the required information from it.

2.2. Optimization Method Design. By combining drones with photoelectric detection, detection can be performed with greater efficiency. Therefore, in order to achieve the purpose of improving the target recognition accuracy of photoelectric detection of UAV, this paper designs an optimization method for the high-precision control device of photoelectric detection of UAV based on POS data. The optimization follows the following principles: before and after optimization, the functions implemented by the control device program are the same; the control algorithm after optimization should run faster or occupy less storage space than before optimization, or both; the optimizer wants the best success at the least cost. The optimization method is shown in Figure 2.

It can be seen from Figure 2 that the method flow is as follows: since the UAV is easily affected by wind during flight, the PID control algorithm is improved and applied to the optimization of UAV control to stabilize the fuselage attitude of the UAV during flight. When the fuselage attitude is stable, the accuracy of photoelectric detection will be improved; then an error correction model is established by analyzing the error source, and finally the original POS data is corrected by the error correction model and applied to the photoelectric detection module of the UAV.

In this process, improving the PID control algorithm is the key point in the optimization method of the photoelectric detection control device of the UAV. A stable body can bring stable detection shooting. This paper mainly improves the controller by improving the control algorithm, which can achieve the purpose of optimizing the fuselage control of the UAV. Achieving the goal requires the following: fast and precise output response, better kinematic characteristics, and static stability characteristics. In the process of building a correction error model, the key point is the analysis of the source of the error. In the process of correcting the original POS data, it is necessary to ensure the comprehensiveness and validity of the data acquisition.

3. Optimize POS Data

3.1. Angle Measurement Model of Photoelectric Detection System. The photoelectric detection system on the UAV can realize the search, tracking, and positioning of the target. The photoelectric detection system adopts the passive working mode; that is, the load operator selects the target area of interest, extracts the target contour through the system, and maintains stable tracking of the target while changing the angle in real time. The measurement data is passed back to the mission console. Through the continuous tracking of the target, a series of measured data of azimuth and inclination

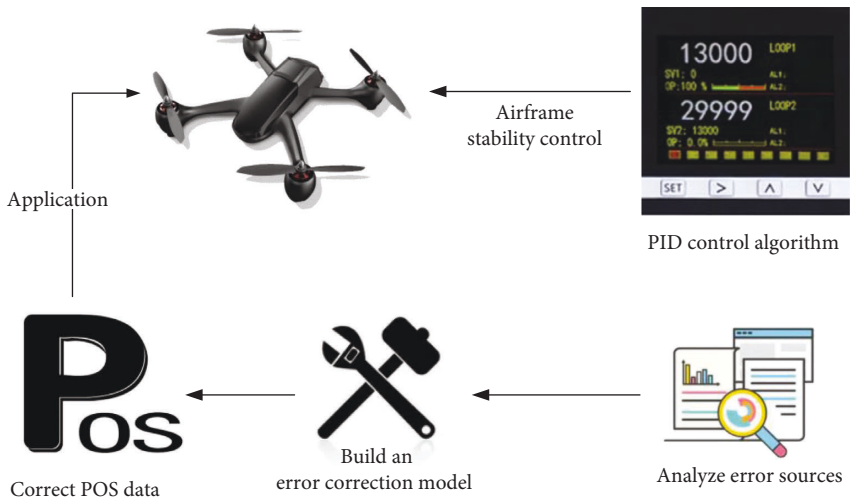

Figure 2: Optimization method for photoelectric detection of UAV.

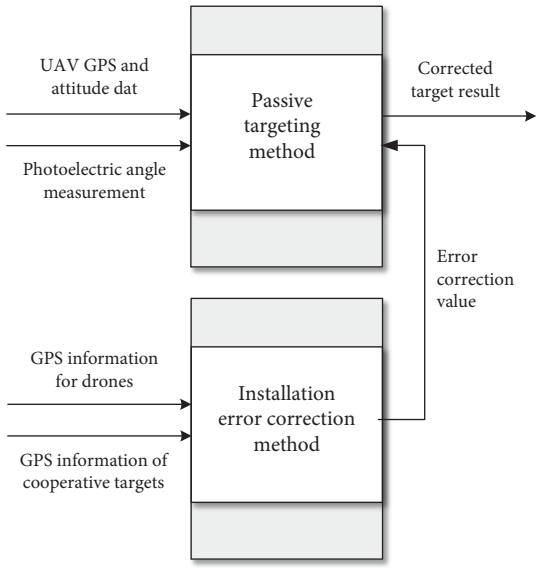

Figure 3: Passive target positioning realization process.

can be obtained. Combining the position data and the position of the flight movement stationary at the relevant moment, the passive positioning method can be used to realize the positioning and calculation of the target parameters. The realization process of passive target positioning is shown in Figure 3.

As shown in Figure 3, the corresponding steps of the passive target positioning realization process are as follows: first, the GPS position information of the UAV and the cooperative target is used to calculate the theoretical azimuth and inclination; second, the measured values of photocharge and inertial force (azimuth and inclination) and UAV navigation data are used to obtain the azimuth and inclination after coordinate transformation; then, the installation error correction value is obtained by the semilinearization method; and finally, the positioning error correction value is applied to the positioning process to complete the target positioning solution.

3.2. Analyze the Source of Errors. In photogrammetry, the transfer model from the lateral body to the normal body is established. The model parameters are solved according to the image points and the corresponding ground points, and the coordinates of the ground control points are obtained. In the image plane coordinates, the origin of the coordinates is usually the point where the main optical axis of the lens intersects the image plane, but this point generally does not coincide with the geometric center of the image, so for the measurement of the image point, first the inner orientation of the acquired image is obtained.

3.3. Monoscopic Space Resection. Spatial separation is a fundamental problem in photometry, and the main idea is to establish a collinear formula of state given the coordinates of several ground control points and the corresponding values of the coordinate measurements of image points. Because the collinear equation is a nonlinear function, it is not conducive to iterative calculation, so it needs to be linearized, expanded according to the first-order term of the Taylor series, and established as the normal equation according to the principle of least squares adjustment.

3.4. System Error Analysis of External Orientation Elements. The exposure position (photography center) of the camera on the drone is not completely coincident with the POS recording position, and there is a certain displacement offset. Therefore, POS data is not strictly an external orientation element of the image. During the photogrammetry process of the UAV, the fixed attitude and state POS data of the UAV can be obtained through the GPS combined system. However, the attitude angle in the POS data does not completely match the outer azimuth element of the orthophoto, so coordinate transformation and system error correction are required. In the subsequent information processing, the electronic method is mainly used. After the optical signal is processed by the photodetector, the optical signal has been converted into an electrical signal. Subsequently, electronic amplifiers,

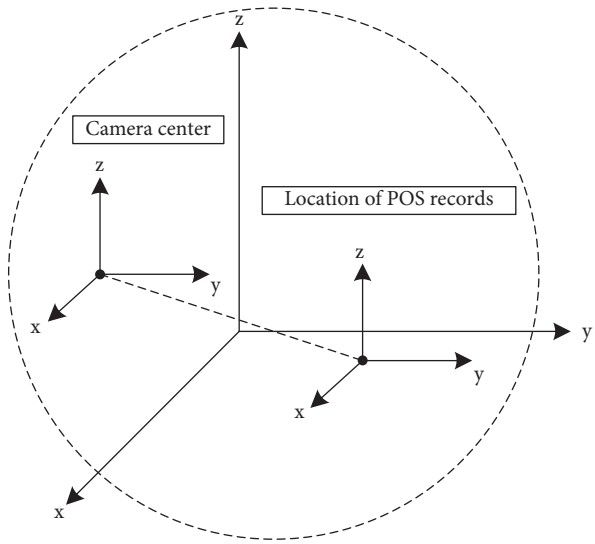

Figure 4: System offset error.

integrated circuits, and computers are used to process the signals. The required information is obtained. The system offset error is shown in Figure 4.

The systematic offset error mainly comes from the offset of the line elements in the outer azimuth. Generally speaking, the drone is approximately parallel to the ground when it flies. However, in the actual process, due to the instability of the aircraft and the influence of air wind, the height of the longitudinal axis will also change. There is a nonnegligible offset. The offset between the POS data and the camera center is shown as

$$\Delta S = \sqrt{\Delta X^2 + \Delta Y^2 + \Delta Z^2}. \tag{1}$$

Among them, X, Y, and Z represent high-order infinitesimal values of the three axes.

3.5. Correct the Original POS Data. On the basis of mastering the sources of systematic errors, an error correction model is designed to correct the original POS data. Main process: available images in the area by performing initial correction and selection of the images obtained by the drone are selected. A small number of control points in the available images are arranged, coordinate transformation on the POS data is performed, and finally a correction model is established. It is assumed that the outer orientation elements of the image are obtained through the solution of ground points, and each image corresponds to the original airborne POS data. The probability distribution is constructed as follows:

$$\begin{bmatrix} \Delta X_i \\ \Delta Y_i \\ \Delta Z_i \\ \Delta \varphi_i \\ \Delta \omega_i \\ \Delta \kappa_i \end{bmatrix} = \begin{bmatrix} X_i - X_{(pos)i} \\ Y_i - Y_{(pos)i} \\ Z_i - Z_{(pos)i} \\ \varphi_i - \varphi_{(pos)i} \\ \omega_i - \omega_{(pos)i} \\ \kappa_i - \kappa_{(pos)i} \end{bmatrix}. \tag{2}$$

Among them, ϕ_i, ω_i, and κ_i represent the attitude angles of the three axes of X_i, Y_i, and Z_i.

Selecting all images for external alignment is complex, time-consuming, and computationally expensive. Therefore, only the error values of the POS data in some images are averaged to correct the overall error, as follows:

$$\begin{cases} \overline{\Delta X}\left(\sum_{i=1}^{n} \Delta X_i\right)/n,\ \overline{\Delta Y} = \left(\sum_{i=1}^{n} \Delta Y_i\right)/n, \\ \overline{\Delta z}\left(\sum_{i=1}^{n} \Delta Z_i\right)/n,\ \overline{\Delta \varphi} = \left(\sum_{i=1}^{n} \Delta \varphi_i\right)/n, \\ \overline{\Delta \omega}\left(\sum_{i=1}^{n} \Delta \omega_i\right)/n,\ \overline{\Delta \kappa} = \left(\sum_{i=1}^{n} \Delta \kappa_i\right)/n. \end{cases} \tag{3}$$

In the formula, $(\overline{\Delta \varnothing}, \overline{\Delta \omega}, \overline{\Delta k})$ is the correction number obtained by the error model. $\Delta\phi$, $\Delta\omega$, and $\Delta\kappa$ represent the attitude angles of the three axes of X, Y, and Z. Finally, according to the different flight trajectories of the UAV flying in space, the positional element errors outside the camera center of the odd-numbered and even-numbered lines of UAV flight are opposite; this will be corrected.

4. Improved PID Control Algorithm

To facilitate the study of the UAV model, the following assumptions are made:

(1) It is assumed that the UAV under experiment is a completely symmetrical, uniform, and rigid body. In the process of photodetection, its elastic deformation and internal force are ignored.

(2) It is assumed that the station center coordinate system is an inertial coordinate system. The influence of the earth's rotation and revolution on the drone is ignored. The curvature of the earth is also ignored and treated as if it were a plane.

(3) It is assumed that the origin of the body coordinate system, the center of mass of the UAV, and the center of the geometric structure coincide.

(4) It is assumed that the gravity and resistance of the UAV flight are not affected by the flight height.

Based on the above research assumptions, formula (4) can be obtained from the Newton–Euler formula:

$$\begin{cases} F = m\dot{v}, \\ M = J\dot{\omega}. \end{cases} \tag{4}$$

Among them, F is the resultant external force on the drone, m is the mass of the drone, $\dot{v}$ is the first derivative of the linear velocity when the drone is flying, M is the moment of momentum when the drone is flying, and J is the rotation of the drone Inertia, and $\dot{\omega}$ is the first derivative of the rotational angular velocity of the drone.

In the body coordinate system, for the UAV, the total lift force is shown as follows:

$$F_{Tb} = \begin{bmatrix} 0 \\ 0 \\ F_1 + F_2 + F_3 + F_4 \end{bmatrix}. \quad (5)$$

Among them, F_1, F_2, F_3, and F_4 are the lift generated by four sets of rotors, respectively.

The matrix expression of the fuselage gravity of the UAV is shown as follows:

$$F_{Ge} = \begin{bmatrix} 0 \\ 0 \\ mg \end{bmatrix}. \quad (6)$$

Among them, g is the acceleration of gravity.

In the station center coordinate system, the air resistance is proportional to the UAV displacement speed, as follows:

$$F_{De} = \begin{bmatrix} K_x \dot{x} \\ K_y \dot{y} \\ K_z \dot{z} \end{bmatrix}. \quad (7)$$

Among them, K_x, K_y, and K_z are the air resistance coefficients of axial displacement motion, respectively.

In summary, the resultant force of the UAV in the station center coordinate system is shown as follows:

$$\sum F_E = F_{Te} - F_{Ge} - F_{De}. \quad (8)$$

In the body coordinate system, ignoring the influence of displacement motion, the UAV performs rotational motion around the body coordinate axis. Its rotational moment is mainly affected by the moments of inertia, angular velocity, air resistance, and gyroscopic effects. The inertia tensor matrix of the UAV rigid body in the body coordinate system is shown as follows:

$$J_b = \begin{bmatrix} J_{xx} & J_{xy} & J_{xz} \\ J_{yx} & J_{yy} & J_{yz} \\ J_{zx} & J_{zy} & J_{zz} \end{bmatrix}. \quad (9)$$

Among them, J_{xx}, J_{yy}, J_{zz} is the moment of inertia and $J_{xy}, J_{xz}, J_{yx}, J_{yz}, J_{zx}, J_{zy}$ is the inertia product. Since the rigid body of the UAV is completely symmetrical, formula (10) can be obtained according to the definition of inertia product:

$$J_{xy} = J_{xz} = J_{yx} = J_{yz} = J_{zx} = J_{zy} = 0. \quad (10)$$

The available UAV inertial matrix is shown as follows:

$$J_b = \begin{bmatrix} J_x & 0 & 0 \\ 0 & J_y & 0 \\ 0 & 0 & J_z \end{bmatrix}. \quad (11)$$

From the differential formula of angular motion, it can be known that the momentum of the UAV is shown as follows:

$$M_b = J_b \dot{\Omega}_b + \Omega_b \times (J_b \Omega_b). \quad (12)$$

Among them, $\dot{\Omega}_b$ is the angular acceleration.

According to the law of conservation of moment of momentum, the resultant moment of UAV rotational motion is shown as follows:

$$\sum M_B = M_b - M_T - M_G. \quad (13)$$

Among them, M_b, M_T, and M_G are the moments in all directions in motion.

The PID algorithm can be expressed as follows:

$$u(t) = K_p e(t) + K_i \int_0^t e(\tau) d\tau + K_d \frac{d}{dt} e(t). \quad (14)$$

The general form of the transfer function of the PID controller is shown as follows

$$G(s) = \frac{U(s)}{E(s)} = K_p \left(1 + \frac{1}{T_i s} + T_d s\right). \quad (15)$$

Among them, T_i is the integral time constant and T_d is the differential time constant.

The proportional control term is mainly concerned with the current error of the system, and the error is multiplied by a positive constant as the output of the proportional term. The output expression of the proportional control term is shown as follows:

$$P_{out} = K_p e(t). \quad (16)$$

The integral control term is mainly concerned with the past errors, and the sum of the error values in the past period of time is multiplied by a positive constant as the integral term output. The output expression of the integral control term is shown as follows:

$$I_{out} = K_i \int_0^t e(t) d\tau. \quad (17)$$

The main concern of the derivative control term is the future error. The first derivative of the error is multiplied by a positive constant as the derivative control term output. The output expression is shown as follows:

$$D_{out} = K_d \frac{d}{dt} e(t). \quad (18)$$

Among them, K_p, K_i, and K_d are all positive constants.

The expression of the positional PID algorithm is shown as follows:

$$u(k) = K_p e(k) + K_i \sum_{j=0}^{k} e(j) + K_d (e(k) - e(k-1)). \quad (19)$$

After further simplification, the final improved PID algorithm is obtained, as follows:

$$\Delta u(k) = K_P \left[\left(1 + \frac{T}{T_i} + \frac{T_d}{T}\right) e(k) - \left(1 + 2\frac{T_d}{T}\right) e(k-1) + \frac{T_d}{T} e(k-2) \right]. \quad (20)$$

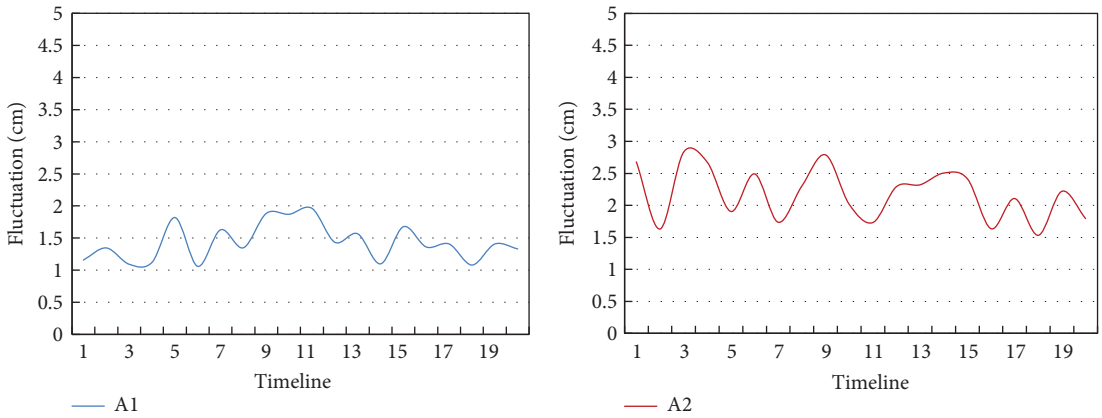

(a) (b)

Figure 5: Hover motion results comparison.

5. Experiment and Result Comparison

According to the above design and research on cascade PID and fuzzy control, this paper uses MATLAB mathematical simulation tool to build and simulate the dynamic model of the UAV flight control system. Based on the corresponding software and hardware facilities, the practical application verification and testing of the UAV flight control algorithm are carried out. The UAV platform is stably controlled by the optimization algorithm of the high-precision control device designed in this paper and the traditional PID algorithm. The high-precision control device optimization algorithm designed in this paper is named A1, and the traditional algorithm is named A2. A comparative experiment was carried out. The experiment was carried out for 20 minutes of UAV photoelectric detection. During the flight movement, by using the open source ground station software, the flight data of the UAV can be detected and adjusted in real time, and the control effect of the UAV attitude control algorithm can be analyzed according to the attitude change curve. The control accuracy and antiinterference ability are verified from the four results of hovering motion results, lateral motion results, photoelectric detection accuracy results, and comprehensive performance results.

5.1. Comparison of Hovering Motion Results. Hovering refers to the flying state in which the UAV keeps its spatial position basically unchanged at a certain height. This flight capability makes the application range of the UAV very wide. It can not only adapt to various complex take-off and landing environments but also engage in various aerial work projects, and even some jobs can only be done by hovering the drone. The comparison of hovering motion results is shown in Figure 5.

Figure 5 shows a comparison of the hovering motion results for the two control device algorithms. In the UAV hovering motion test using the high-precision control device optimization algorithm designed in this paper, the offset of the fuselage from the origin within 20 minutes is between 1.06 and 1.96 cm; in the drone hovering motion test using the traditional control device algorithm, the offset of the fuselage from the origin within 20 minutes is between 1.53 and 2.83 cm. The high-precision control device optimization algorithm designed in this paper is far superior to the traditional control device algorithm in hovering motion.

5.2. Comparison of Lateral Motion Results. The lateral motion of the UAV is mainly manifested in three motion modes, namely, the Dutch roll mode, the fast roll mode, and the helical mode. In the Dutch roll mode, the torque related to the rotation is interrelated; in the fast roll-on mode, the roll angular velocity causes the yaw moment, and the yaw angular velocity causes the roll moment. In helical mode, coordinated turns can be controlled by increasing the damping of the rolling motion. In this experiment, the motion modes of the UAV under the two control device algorithms are tested, and the comparison results are shown in Figure 6.

Figure 6 shows a comparison of the lateral motion results of the two control device algorithms. In the lateral motion test of the UAV using the high-precision control device optimization algorithm designed in this paper, the number of completed lateral motion cycles of the fuselage per minute is between 6 and 9 times within 20 minutes; in the hovering motion test of the UAV using the traditional control device algorithm, the number of completed lateral motion cycles of the fuselage per minute within 20 minutes is between 4 and 6 times. The high-precision control device optimization algorithm designed in this paper is far superior to the traditional control device algorithm in lateral motion.

5.3. Comparison of Photoelectric Detection Accuracy Results. The photoelectric detection system on the UAV can realize the search, tracking, and positioning of the target. The photoelectric detection system adopts the passive working mode; that is, the target area is selected by the load operator, and the target contour is extracted by the system. While maintaining stable tracking of the target, the angle

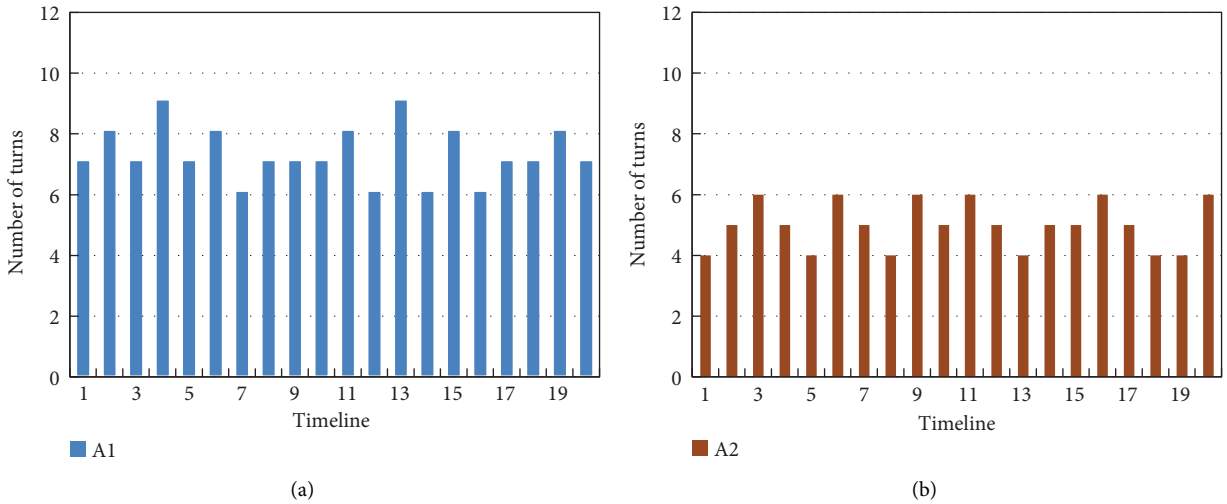

Figure 6: Lateral motion results comparison.

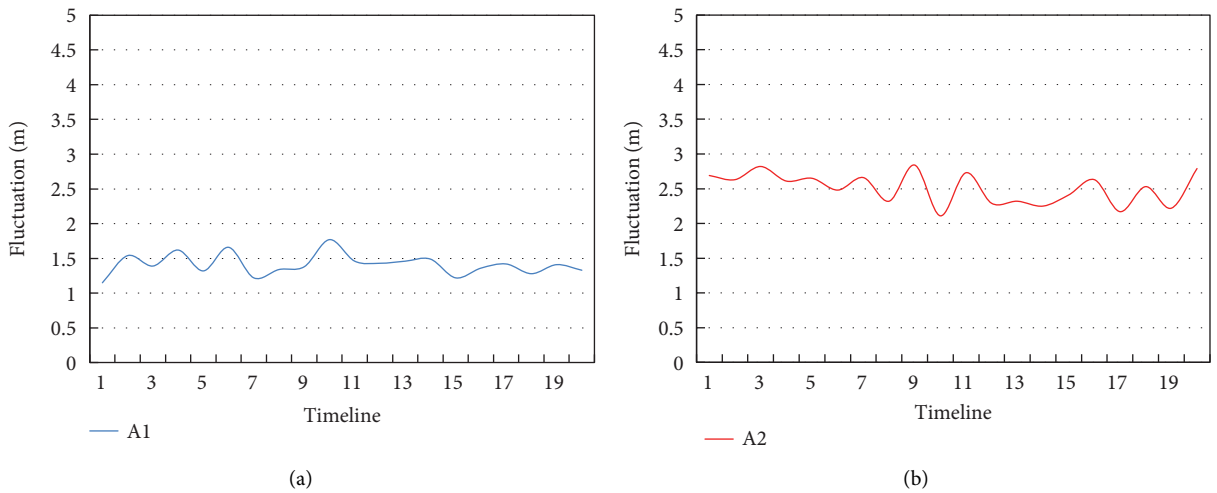

Figure 7: Comparison of photoelectric detection accuracy results.

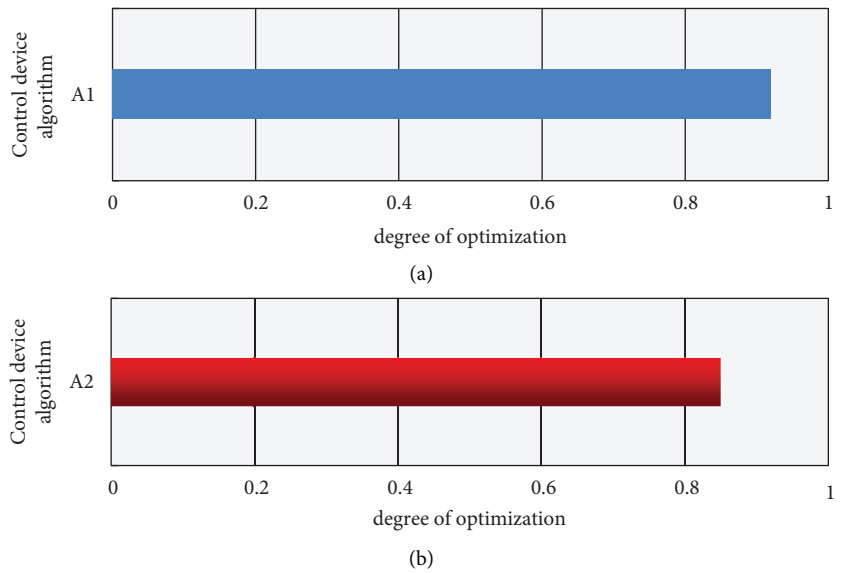

Figure 8: Final result comparison.

measurement data is transmitted back to the mission console in real time. The photoelectric detection accuracy results are shown in Figure 7.

Figure 7 shows the comparison of the photodetection accuracy results of the two control device algorithms. In the UAV photoelectric detection accuracy test using the high-precision control device optimization algorithm designed in this paper, the deviation between the detection locking point and the target within 20 minutes is between 1.15 and 1.77 cm; in the UAV photoelectric detection accuracy test using the traditional control device algorithm, the offset of the fuselage from the origin within 20 minutes is between 2.11 and 2.84 cm. The high-precision control device optimization algorithm designed in this paper is far superior to the traditional control device algorithm in terms of photoelectric detection accuracy.

5.4. Comparison of Comprehensive Performance Results. Finally, the comprehensive performance comparison results of the two control device algorithms are obtained, as shown in Figure 8.

Figure 8 shows a comparison of the overall performance results of the two control device algorithms. The comprehensive performance score of the optimization algorithm of the high-precision control device designed in this paper is 0.92 points, and the comprehensive performance score of the traditional control device algorithm is 0.85 points. The performance of the high-precision control device optimization algorithm designed in this paper is far superior to that of the traditional control device algorithm. The performance has improved by about 8.23%.

6. Conclusion

The combination of a UAV and a photoelectric detection system can flexibly and conveniently carry out photoelectric detection. However, due to the system error of the algorithm and various other objective factors, the potential of the optoelectronic equipment has not been fully exerted, and the control accuracy of the optoelectronic detection is low. Through experiments, four results were obtained, including hovering motion results, lateral motion results, photoelectric detection accuracy results, and comprehensive performance results.

Data Availability

The data that support the findings of this study are available from the corresponding author upon request.

Conflicts of Interest

The authors declare that they have no conflicts of interest.

References

[1] K. He, H. Hong, and G. Jiang, "Analysis of assembly error effect on stability accuracy of unmanned aerial vehicle photoelectric detection system," *Applied Sciences*, vol. 10, no. 7, pp. 2311–2352, 2020.

[2] J. Escobar and S. Sandoval, "Unmanned aerial vehicle (UAV) for sea turtle skeleton detection in the Mexican Pacific," *Remote Sensing Applications Society and Environment*, vol. 1, no. 1, pp. 4–12, 2021.

[3] J. Ren and X. Jiang, "Regularized 2-D complex-log spectral analysis and subspace reliability analysis of micro-Doppler signature for UAV detection," *Pattern Recognition*, vol. 69, no. 4, pp. 225–237, 2017.

[4] A. Thomas, T. A. Alexandra, and P. X. Eirini, "Novelty detection classifiers in weed mapping: Silybum marianum detection on UAV multispectral images," *Sensors*, vol. 17, no. 9, pp. 2007–2145, 2017.

[5] O. T. Damian, H. L. David, and B. Rocio, "Automatic hotspot and sun glint detection in UAV multispectral images," *Sensors*, vol. 17, no. 10, pp. 2352–2484, 2017.

[6] C. A. Kerrache, A. Lakas, and N. Lagraa, "UAV-assisted technique for the detection of malicious and selfish nodes in VANETs," *Vehicular Communications*, vol. 11, no. 6, pp. 1–11, 2018.

[7] P. Martinez and M. Barczyk, "Implementation and optimization of the cascade classifier algorithm for UAV detection and tracking," *Journal of Unmanned Vehicle Systems*, vol. 7, no. 4, pp. 296–311, 2019.

[8] J. Li, J. Fang, and Z. Lu, "Airborne position and orientation system for aerial remote sensing," *International Journal of Aerospace Engineering*, vol. 2017, no. 1, pp. 1–11, 2017.

[9] X. Niu, T. Liu, and J. Kuang, "A novel position and orientation system for pedestrian indoor mobile mapping system," *IEEE Sensors Journal*, vol. 21, no. 2, pp. 2104–2114, 2021.

[10] W. Ye, B. Gu, and Y. Wang, "Airborne distributed position and orientation system transfer alignment method based on fiber bragg grating," *Sensors*, vol. 20, no. 7, p. 2120, 2020.

[11] J. Li, S. Zou, B. Gu, and J. Fang, "Adaptive two-filter smoothing based on second-order divided difference filter for distributed position and orientation system," *Science China(Information Sciences)*, vol. 62, no. 9, pp. 130–143, 2019.

[12] X. Gong and L. Chen, "A conditional cubature Kalman filter and its application to transfer alignment of distributed position and orientation system," *Aerospace Science and Technology*, vol. 95, no. 3, pp. 105–405, 2019.

[13] Z. Zhu, Y. Guo, and W. Ye, "A real-time gravity compensation method for a high-precision airborne position and orientation system based on a gravity map," *Journal of Navigation*, vol. 71, no. 3, pp. 711–728, 2018.

[14] K. Takashima, T. Okazaki, and K. Toyoda, "Magnetic sensor system for detecting position and orientation of an endocranial catheter tip(Imaging & Measurement)," *Work*, vol. 411, no. 6, pp. 258–265, 2017.

[15] E. Langbehn, F. Steinicke, and M. Lappe, "In the blink of an eye - leveraging blink-induced suppression for imperceptible position and orientation redirection in virtual reality," *ACM Transactions on Graphics*, vol. 37, no. 4, pp. 1–11, 2018.

[16] C. Zhang and Z. Wei, "Spectrum sharing for drone networks," *IEEE Journal on Selected Areas in Communications*, vol. 35, no. 1, pp. 136–144, 2017.

[17] J. Wang and Q. Ping, "Photodetection-induced relative timing jitter in synchronized time-lens source for coherent Raman scattering microscopy," *Journal of Innovative Optical Health Sciences*, vol. 10, no. 5, pp. 16–21, 2017.

[18] B. Ding and G. Wen, "Sparsity constraint nearest subspace classifier for target recognition of SAR images," *Journal of Visual Communication and Image Representation*, vol. 52, no. 6, pp. 170–176, 2018.

[19] X. Qi, N. Wu, and H. Wang, "A factor graph-based iterative detection of faster-than-Nyquist signaling in the presence of phase noise and carrier frequency offset," *Digital Signal Processing*, vol. 63, no. 7, pp. 25–34, 2017.

[20] D. V. Gorbatov, V. A. Konyshev, and T. O. Lukinykh, "Effect of anisotropy of a single-mode fibre on lightning-induced rotation of polarisation of a light signal in an optical ground wire," *Quantum Electronics*, vol. 52, no. 1, pp. 87–93, 2022.